

# Journal of Visualized Experiments

## Use of Principal Components for Scaling Up Topographic Models to Map Soil Redistribution and Soil Organic Carbon

--Manuscript Draft--

<b>Article Type:</b>	Invited Methods Article - JoVE Produced Video
<b>Manuscript Number:</b>	JoVE58189R3
<b>Full Title:</b>	Use of Principal Components for Scaling Up Topographic Models to Map Soil Redistribution and Soil Organic Carbon
<b>Keywords:</b>	Topography-based model; stepwise principal component regression; stepwise ordinary linear regression; digital elevation model; soil redistribution; soil organic carbon.
<b>Corresponding Author:</b>	Greg McCarty "USDA-ARS Beltsville Agricultural Research Center" Beltsville, MD UNITED STATES
<b>Corresponding Author's Institution:</b>	"USDA-ARS Beltsville Agricultural Research Center"
<b>Corresponding Author E-Mail:</b>	Greg.McCarty@ars.usda.gov
<b>Order of Authors:</b>	Xia Li Greg McCarty
<b>Additional Information:</b>	
<b>Question</b>	<b>Response</b>
Please indicate whether this article will be Standard Access or Open Access.	Open Access (US\$4,200)
Please indicate the <b>city, state/province, and country</b> where this article will be <b>filmed</b> . Please do not use abbreviations.	10300 Baltimore Ave, Beltsville, MD 20705



United States Department of Agriculture

---

Research, Education, and Economics  
Agricultural Research Service

**Use of Principal Components for Scaling Up Topographic Models to Map Soil Redistribution and Soil Organic Carbon**

Dear Dr. Phillip Steindel,

We are resubmitting our revised manuscript entitled "Use of Principal Components for Scaling Up Topographic Models to Map Soil Redistribution and Soil Organic Carbon" (Original Manuscript #: JoVE58189R2) for consideration by *JoVE*. In the revised manuscript, we addressed editorial comments, and outlined our response to each comment in the attached "rebuttal letter". We also provide a latest version, and a marked-up version of the manuscript to highlight our revisions.

Please feel free to contact me if you have any questions regarding our revision.

We are thankful for your consideration.

Best regards.

A handwritten signature in black ink, reading "Greg McCarty", is positioned above the typed name.

Greg McCarty

Soil Scientist

E-mail : [greg.mccarty@ars.usda.gov](mailto:greg.mccarty@ars.usda.gov)

Tel.: +1 301-504-7401

Hydrology & Remote Sensing Laboratory  
Beltsville Agricultural Research Center  
Bldg. 007, Room 127  
10300 Baltimore Avenue  
Beltsville, Maryland 20705  
USDA is an Equal Opportunity Employer

**TITLE:****Use of Principal Components for Scaling Up Topographic Models to Map Soil Redistribution and Soil Organic Carbon****AUTHORS AND AFFILIATIONS:**

Xia Li<sup>1,2</sup>, Gregory W. McCarty<sup>2</sup>

<sup>1</sup>Department of Geographical Sciences, University of Maryland, College Park, MD, USA

<sup>2</sup>Hydrology & Remote Sensing Laboratory, Agricultural Research Service, United States Department of Agriculture, Beltsville, MD, USA

**Corresponding Author:**

Gregory W McCarty (greg.mccarty@ars.usda.gov)

**Email Address of Co-author:**

Xia Li (xiali626@umd.edu)

**KEYWORDS:**

Topography-based model, stepwise principal component regression, stepwise ordinary linear regression, digital elevation model, soil redistribution, soil organic carbon

**SUMMARY:**

Landscape processes are critical components of soil formation and play important roles in determining soil properties and spatial structure in landscapes. We propose a new approach using stepwise principal component regression to predict soil redistribution and soil organic carbon across various spatial scales.

**ABSTRACT:**

Landscape topography is a critical factor affecting soil formation and plays an important role in determining soil properties on the earth surface, as it regulates the gravity-driven soil movement induced by runoff and tillage activities. The recent application of Light Detection and Ranging (LiDAR) data holds promise for generating high spatial resolution topographic metrics that can be used to investigate soil property variability. In this study, fifteen topographic metrics derived from LiDAR data were used to investigate topographic impacts on redistribution of soil and spatial distribution of soil organic carbon (SOC). Specifically, we explored the use of principal components (PCs) for characterizing topography metrics and stepwise principal component regression (SPCR) to develop topography-based soil erosion and SOC models at site and watershed scales. Performance of SPCR models was evaluated against stepwise ordinary least square regression (SOLSR) models. Results showed that SPCR models outperformed SOLSR models in predicting soil redistribution rates and SOC density at different spatial scales. Use of PCs removes potential collinearity between individual input variables, and dimensionality reduction by principal component analysis (PCA) diminishes the risk of overfitting the prediction models. This study proposes a new approach for modeling soil redistribution across various spatial scales. For one application, access to private lands is often limited, and the need to extrapolate findings from representative study sites to larger settings that include private lands

can be important.

## **INTRODUCTION:**

Soil redistribution (erosion and deposition) exerts significant impacts on soil organic carbon (SOC) stocks and dynamics. Increasing efforts have been devoted to investigating how SOC is detached, transported, and deposited over the landscape<sup>1-3</sup>. Carbon (C) sequestration and SOC distribution are influenced by gravity-driven soil movement induced by water erosion<sup>4-6</sup>. In cultivated fields, soil translocation by tillage is another important process contributing to C redistribution<sup>7-9</sup>. Tillage erosion causes a considerable net downslope movement of soil particles and leads to a within-field soil variation<sup>10</sup>. Both water and tillage erosion are significantly affected by landscape topography, which determines the locations of erosional and depositional sites<sup>11</sup>. Therefore, effective soil erosion regulation and C dynamic investigation in agricultural lands calls for a better understanding of topographic controls on soil erosion and movements.

Several studies have investigated the impacts of topography on soil redistribution and associated SOC dynamics<sup>9,12-17</sup>. Van der Perk *et al.*<sup>12</sup> reported that topographic factors explained 43% of variability in soil redistribution. Rezaei and Gilkes<sup>13</sup> found higher SOC in soils on a shady aspect, due to lower temperatures and less evaporation when compared to other aspects in rangelands. Topography may have more significant impacts on soil redistribution in agricultural lands with traditional tillage treatment than those with minimum tillage, due to the interactions between landforms and tillage practices<sup>9</sup>. However, these findings were primarily derived from field observations, which present difficulties in investigating soil properties at a broader spatial scale. There is a pressing need to develop new strategies to effectively understand spatial patterns of soil properties at watershed and regional scales.

The objective of this study is to develop efficient models to simulate soil redistribution and SOC distribution. Topography-based models using topographic metrics as predictors have been developed to quantify soil erosion and deposition processes. Compared with empirical- or process-based erosion models that employed discrete field samplings to simulate soil erosion<sup>18,19</sup>, topography-based models could be developed based on topographic information derived from digital elevation models (DEMs) with high resolutions. This approach allows for continuous soil property simulations at the watershed or regional scale. In the past several decades, accuracy of topographic information has substantially improved, with increasing availability of high resolution remotely sensed data. Although previous studies have employed topography-based models to simulate soil properties<sup>12,20-22</sup>, most of these investigations used a single topographic metric or single category of topographic metrics (local, non-local, or combined topographic metrics), which may not have sufficiently explored topographic impacts on soil microbial activity. Therefore, to gain a better understanding of topography controls on soil erosion and C dynamics, we examined a comprehensive set of topographic metrics including local, non-local, and combined topographic metrics and developed multi-variable topography-based models to simulate soil property dynamics. Applications of these models are expected to provide scientific support for better soil erosion control and agricultural land management.

Topographic metrics are generally categorized into one of three categories: a) local topographic metrics, b) non-local topographic metrics, or c) combined topographic metrics. Local topographic metrics refer to local features of one point on the land surface. Non-local topographic metrics refer to the relative locations of selected points. Combined topographic metrics integrate local and non-local topographic metrics. A set of topographic metrics affecting soil erosion and deposition were used in this study to investigate the topographic controls on soil movement and C stocks (**Table 1**). Specifically, we used four local topographic metrics [slope, profile curvature (P\_Cur), plan curvature (PI\_Cur), general curvature (G\_Cur)], seven non-local topographic metrics [flow accumulation (FA), topographic relief, positive openness (POP), upslope slope (UpSI), flow path length (FPL), downslope index (DI), catchment area (CA)], and three combined topographic metrics [topographic wetness index (TWI), stream power index (SPI), and slope length factor (LS)].

## PROTOCOL:

### 1. Topographic Analyses

#### 1.1. Digital data preprocess

1.1.1. Collect LiDAR data from the GeoTREE LiDAR mapping project website. Select “boundary type” and “region” to zoom into a specific area. Draw a polygon to download LiDAR tiles for the selected study area.

1.1.2. Convert the raw LiDAR data to a LAS file using the geographic information system (GIS) mapping tool.

1.1.3. Generate DEMs with a 3-m spatial resolution using inverse distance weighted interpolation.

1.1.4. Filter the 3-m DEMs twice with a 3-kernel low pass filter to reduce noises associate with local variation.

#### 1.2. Topographic metric generation

1.2.1. To generate topographic metrics, first download the latest version of the System for Automated Geoscientific Analysis (SAGA)<sup>23</sup>. Click “Import Raster” in the Import/Export section to import the filtered 3-m DEMs into SAGA.

1.2.2. Click the “Slope, Aspect, Curvature” module of SAGA with the default settings to generate the slope and curvature-related [profile curvature (P\_Cur), plan curvature (PI\_Cur), and general curvature (G\_Cur)] metrics using the filtered DEMs (**Figure 1**).

1.2.3. Click the “Flow Accumulation (Top-Down)” module of SAGA and select “Deterministic infinity” as the method to generate flow accumulation (FA) metric using the filtered DEMs.

1.2.4. Click the “SAGA Topographic Openness” module with the default settings to generate the positive openness (POP) metric using a filtered z-axis amplified image.

1.2.5. Click the “LS- factor (Field Based)” module of SAGA with the default settings to generate the upslope slope (Upsl) and slope length factor (LS\_FB) metrics using the filtered DEMs.

1.2.6. Click the “Flow Path Length” module of SAGA with the default settings to generate the flow path length (FPL) metric using the filtered DEMs.

1.2.7. Click the “Downslope Distance Gradient” module of SAGA with the default settings to generate the downslope index (DI) metric using the filtered DEMs.

1.2.8. Click the “SAGA Wetness Index” module and select “absolute catchment area” as the Type of Area to generate the catchment area (CA) and topographic wetness index (TWI) metrics using the filtered DEMs.

1.2.9. Click the “Stream Power Index” module of SAGA and select “pseudo specific catchment area” as the Area Conversion to generate the stream power index (SPI) metric using the filtered DEMs.

1.2.10. Generate maximum elevation maps with multiple radiuses. Filter the maximum elevation maps twice through a 3-kernel low pass filter. Subtract the filtered 3-m DEM from the filtered maximum elevation maps to obtain a series of relief maps. Extract a series of relief variables to a number of locations.

1.2.11. Perform principal component analysis (PCA) on the relief variables to convert the reliefs into topographic relief components. Select principal components that explain more than 90% variance of the relief dataset as the topographic relief metrics.

## **2. Field Data Collection**

### **2.1. Field sampling**

2.1.1. Select a number of cropland field locations that can adequately represent the landscape characteristics of the study area and several representative small-scale cropland fields that can be intensively sampled.

Note: The soil samples collected from the two cropland fields were used for model calibration. Soil samples collected from the entire study area were used for model validation.

2.1.2. Upload all the sample location coordinates to a code-based geographic positioning system (GPS) and physically locate them in the fields.

2.1.3. Collect 3 samples for each sampling location from the top 30 cm soil layer using a push

probe (3.2 cm in diameter).

Note: Soil samples from 30-50 cm layers were collected at sites where sediment deposition was expected. The volume of each sample was 241 cm<sup>3</sup>.

2.1.4. Record geographic coordinate information of sampling locations using GPS.

2.1.5. Weigh the soil samples after drying them at 90 °C for 48 h. Calculate soil density using information of total sample volumes at sampling locations and weights. Mix the three samples from the same location to get a composite soil sample.

## 2.2. Soil sample preparation

2.2.1. Sieve the composite soil samples with a 2-mm screen.

2.2.2. Grind a 20 g subsample of the sieved soil to a very fine powder with a roller mill.

## 2.3. Soil sample analyses

2.3.1. Measure soil total carbon (C) content in roller milled samples through combustion on a CN elemental analyzer at a temperature of 1350 °C. Estimate calcium carbonate C content by analyzing the remaining C after baking soil organic matter at a temperature of 420 °C for 16 h in a furnace.

2.3.2. Calculate SOC content (%) by subtracting calcium carbonate C content from total soil C content. Convert SOC content (%) to SOC density (kg m<sup>-2</sup>) using soil density.

2.3.3. Put the bulk 2-mm sieved soil samples in Marinelli beakers and seal them. Measure <sup>137</sup>Cs concentration of each sample through gamma-ray analysis using a spectroscopy system that receives inputs from three high purity coaxial germanium crystals (HpCN30% efficiency) into 8192-channel analyzers (see **Table of Materials**).

2.3.4. Calibrate the system using an analytic mixed radionuclide standard<sup>11</sup>. Convert <sup>137</sup>Cs concentration to <sup>137</sup>Cs inventory using soil density.

2.3.5. Calculate soil redistribution rate using <sup>137</sup>Cs inventory by applying the Mass Balance Model II (MBMII) in a spreadsheet add-in program developed by Walling *et al.*<sup>24</sup>.

## 3. Topography-Based Model Development

### 3.1. Topographic principal component estimation

3.1.1. Extract the topographic metrics for sampling locations in the entire study area and the small-scale cropland fields.

3.1.2. Standardize the topographic metrics of the sampling locations in the entire study area by using mean and standard deviation. Estimate the topographic metric loadings in each component based on the standardized topographic metrics using PCA with statistical software package. Collect the topographic metric loadings in each topographic principal component (TPC) and select the top TPCs that explain 90% variance of all metrics.

3.1.3. Standardize the topographic metrics of the sampling locations in the small-scale cropland fields. Calculate the top TPCs for each location by sum of the standardized topographic metrics weighted by the corresponding loadings from the sampling locations in WCW.

### 3.2. Model calibration

3.2.1. Perform stepwise ordinary least square regression (SOLSR) to develop topography-based SOLSR<sub>f</sub> models for SOC density and soil redistribution rates based on all topographic metrics at the small-scale cropland fields. Use Akaike information criterion (AIC) and leave-one-out cross-validation to select the optimal combination of topographic metrics for the best-fitted SOLSR<sub>f</sub> models.

3.2.2. Check the collinearity among the topographic variables using the variance inflation factor (VIF). Remove the variables with the largest VIF ( $VIF \geq 7.5^{25}$ ), and check VIF again. Remove the variables until the VIFs of all variables are  $< 7.5$ . Perform SOLSR to develop topography-based SOLSR<sub>r</sub> models for SOC density and soil redistribution rates based on topographic metrics that were removed high collinearity variables. Use the AIC and leave-one-out cross-validation to select the optimal combination for the best-fitted SOLSR<sub>r</sub> models.

3.2.3. Perform stepwise principal component regression (SPCR) to develop topography-based SPCR models for SOC density and soil redistribution rates based on the TPCs at the small-scale cropland fields. Use the AIC and leave-one-out cross-validation to select the optimal combination of TPCs for the best-fitted SPCR models.

3.2.4. Calculate the adjusted coefficient of determination ( $R_{adj}^2$ ), Nash-Sutcliffe efficiency (NSE), and ratio of the root mean square error to the standard deviation of measured data (RSR) to assess model efficiencies.

### 3.3. Model evaluation

3.3.1. Estimate SOC density and soil redistribution rates in the entire study area by applying the estimated models.

3.3.2. Validate the developed model by comparing prediction with measured dataset of SOC density and soil redistribution rates in the entire study area. Evaluate the model performances using  $R_{adj}^2$ , NSE, and RSR values.



## REPRESENTATIVE RESULTS:

We used the Walnut Creek Watershed (WCW) as a testbed to assess feasibility of topography-based models in investigating soil redistribution and SOC dynamics. The watershed is in Boone and Story counties within the state of Iowa (41°55′-42°00′N; 93°32′-93°45′W) with an area of 5,130 ha (**Figure 2**). Croplands is the dominant land use type in the WCW, with a relatively flat terrain (mean 90 m, topographic relief 2.29 m). Chisel plowing, disking, and harrowing operations are the principal tillage practices in the crop fields<sup>26,27</sup>; however, tillage directions vary due to differences in management practices.

Four hundred and sixty crop field locations were randomly selected to derive topographic information in the WCW (**Figure 2**). 100 out of the 460 locations, including two 300 m transects (each have 9 sampling locations), were selected to conduct field samplings and for analysis of SOC and soil redistribution levels. In addition, two small-scale field sites with topographic landscape, soil types, and tillage practices similar to the WCW were selected for more intensive samplings. At each small-scale field site, a 25 × 25 m grid cell was created, and 230 sampling locations were located at grid nodes (**Figure 3**). Topographic metrics and soil property information were calculated for the 230 locations.

The topographic metrics in the WCW were generated following the above protocol. The WCW is characterized with low-to-moderate topography (elevation ranging from 260 to 325 m) with a relative low slope (ranging from 0 to 0.11 radian), upslope slope (0 to 0.09 m), and moderate curvatures (profile curvature: -0.009 to 0.009 m<sup>-1</sup>, plan curvature: -0.85 to 0.85 m<sup>-1</sup>, general curvature: -0.02 to 0.02 m<sup>-1</sup>). The vertical elevations of DEMs were enlarged 100 times to increase the distinguishability of the relatively low field-scale relief found in the WCW for creating the positive openness metrics (POP100). After conversion, the range of positive openness increased from 0.08 radians (POP: 1.51-1.59 radians) to 0.86 radians (POP100: 0.36-1.22 radians).

For the topographic relief, we generated seven relief maps with following radiuses: 7.5 m, 15 m, 30 m, 45 m, 60 m, 75 m, and 90 m. Two relief principal components were selected based on results of PCA on the seven relief variables. The first showed coarse resolution relief variation with relief<sub>45m</sub> as the main variable. We defined this component as the large-scale relief (LsRe). The second component, which was highly correlated with relief<sub>7.5m</sub> and presented fine resolution relief variation, was defined as the small-scale relief (SsRe).

Results of correlation analyses between topographic metrics and SOC density/soil redistribution are presented in **Table 2**. The TWI and LsRe showed the highest correlations with SOC density and soil redistribution rates, respectively. Spatial patterns of the two metrics are presented in **Figure 4**. Details of the TWI and LsRe can be better observed from the transect area. Both metrics showed high values in depressional area and low values in sloping and ridge areas. However, differences between the two metrics occurred in ditch areas, where the TWI exhibited extremely high values but the values of LsRe were not different from adjacent areas.

After generating the fifteen topographic metrics, we used PCA on these topographic variables over the 460 sampling sites in the WCW. The first seven topographic principal components (TPCs)

that explained more than 90% variability of the whole topographic dataset were selected. Five TPCs that were final selected to build topography-based models are listed in **Table 3**. For the first principal component (TPC1), G\_Cur showed the highest loading. Slope, TWI, Upsl, and LS\_FB were the most important metrics in TPC2, with loadings larger than 0.35. In the TPC3, FA, SPI, and CA were important metrics, with loadings of 0.482, 0.460, and 0.400, respectively. FPL (-0.703) and Pl\_Cur (0.485) were the most important in the TPC6. The main metrics with high loadings in the TPC7 were SsRe (0.597), DI (0.435), FPL (0.407), and Pl\_Cur (0.383).

Collinearity of topographic variable was checked by examining VIF. Of the 15 metrics, slope, TWI, and G\_Cur were removed due to the high VIFs. Based on soil redistribution rates and carbon density data from sites 1 and 2, SOLSR models were developed using all 15 metrics (SOLSR<sub>f</sub>) and the 12 metrics with collinear covariate removed (SOLSR<sub>r</sub>) (**Table 4**). Generally, over 70% and 65% of variability in SOC density and soil redistribution rates were explained by the SOLSR<sub>f</sub> models, respectively. For the models with collinear covariate removed (SOLSR<sub>r</sub>), simulation efficiencies were slightly lower than SOLSR<sub>f</sub> models (68% for SOC density and 63% for soil redistribution). NSEs were slightly lower and RSR were slightly higher in SOLSR<sub>r</sub> models than in SOLSR<sub>f</sub> models.

For SPCR models, similar simulation efficiencies as SOLSR<sub>r</sub> are observed in **Table 4**. However, fewer independent variables were selected in SPCR models (less than 5 variables) than the SOLSR<sub>f</sub> and SOLSR<sub>r</sub> models (more than 6 variables). TPCs 1, 2, 3, and 7 were selected as the independent variable combinations for the SOC model and TPCs 1, 2, 3, 6, and 7 were selected as the combination for the soil redistribution model.

We found that the SPCR models had the best predictions and the SOLSR<sub>r</sub> models showed the poorest performances at the watershed scale. The coefficients of determination ( $r^2$ ) by comparing SOC density prediction to observation increased from: 1) 0.60 in SOLSR<sub>f</sub> and 0.52 in SOLSR<sub>r</sub> to 0.66 in SPCR, and 2) NSE increased from 0.21 in SOLSR<sub>f</sub> and 0.16 in SOLSR<sub>r</sub> to 0.59 in SPCR; while RSR reduced from 0.87 in SOLSR<sub>f</sub> and 0.91 in SOLSR<sub>r</sub> to 0.64 in SPCR. Soil redistribution rate prediction in SPCR accounted for 36% of the variability in the measured variable and was higher than the predictions by SOLSR<sub>f</sub> (34%) and SOLSR<sub>r</sub> (0.35%). A higher NSE and lower RSR in SPCR (NSE = 0.33, RSR = 0.82) compared to SOLSR<sub>f</sub> (NSE = 0.31, RSR = 0.83) and SOLSR<sub>r</sub> (NSE = 0.32, RSR = 0.82) also demonstrated a better performance in soil redistribution rate simulation by SPCR.

According to the model performance evaluations, SPCR models were selected to generate SOC density and soil redistribution rate maps at the watershed scale. The maps revealed consistent patterns between model simulations and field measurements (**Figure 5**). The high consistencies between simulations and observations were more evident along the transects. Both SOC density and soil redistribution rates showed high correlations with landscape topography. High values of SOC density can be found in footslope and depositional areas, where soil deposition occurred, while low values of SOC density were observed in sloping areas, where soil erosion took place.

#### FIGURE AND TABLE LEGENDS:

**Figure 1: The Slope, Aspect, Curvature module in the System for Automated Geoscientific**

**Analysis (SAGA).** The polygons show the locations of study areas.

**Figure 2: Location of Walnut Creek Watershed and sampling sites in the watershed (Iowa).** This figure was adapted from previous work<sup>17</sup>.

**Figure 3: Location of sampled sites a) 1 and b) 2 (z-axis 15x elevation).** This figure was adapted from previous work<sup>17</sup>.

**Figure 4: Topographic metric maps.** (a) Topographic wetness index (TWI) and (b) large-scale topographic relief (LsRe) in the Walnut Creek Watershed and transect area (z-axis 15 x elevation).

**Figure 5: Soil redistribution rate ( $\text{t ha}^{-1} \text{ year}^{-1}$ ) maps and SOC density ( $\text{kg m}^{-2}$ ) maps.** Shown are soil redistribution maps (a) within the Walnut Creek Watershed and (b) along two transects. Shown are SOC density ( $\text{kg m}^{-2}$ ) maps (c) within the Walnut Creek Watershed and (d) along two transects using the stepwise principal component analysis models (z-axis 15x elevation).

**Table 1: Significances of selected topographic metrics.**

**Table 2: Spearman's rank correlation ( $n = 560$ ) between selected topographic metrics and soil organic carbon (SOC) density and soil redistribution rates (SR).**

**Table 3: Variable loadings in the principal components (PCs) calculated for topographic metrics ( $n = 460$ ) in Walnut Creek Watershed.**

**Table 4: Models of soil organic carbon (SOC) density and soil redistribution rates (SR) for agricultural fields based on topographic metrics at sites 1 and 2.**

## **DISCUSSION:**

The SOLSR<sub>f</sub> models had slightly better performances than the SPCR models in calibration at the field scale. However, some of the topographic metrics, such as SPI and CA ( $r > 0.80$ ), are closely correlated with each other. The collinearity may add uncertainties to model predictions. Because of the multicollinearity among predictors, small changes in the input variables can significantly affect the model predictions<sup>41</sup>. Therefore, the SOLSR<sub>f</sub> models tended to be unstable and showed low efficiencies in simulations of SOC density and soil redistribution rate at the watershed scale. The SPCR models substantially outperformed the SOLSR<sub>f</sub> models in prediction of SOC distribution at the watershed scale. TPCs eliminate the multicollinearity by converting the fifteen topographic metrics into mutually independent (orthogonal) components. The conversion also uncovered underlying relationships among topographic metrics. As indicated by the high loadings ( $> 0.35$ ) of topographic metrics to the components, the TPC1, TPC2, TPC3, TPC6, and TPC7 were associated with runoff velocity, soil water content, runoff volume, flow divergence, and flow acceleration, respectively. Spatial patterns of soil redistribution rates and SOC distribution were highly correlated with soil water content and runoff divergence in the WCW, which is consistent with the study of Fox and Papanicolaou<sup>2</sup>, which demonstrated that eroded soil from upland could be impacted by flow divergence in a low-relief agricultural watershed.

Moreover, fewer predictor variables in the SPCR models than the SOLSR<sub>f</sub> and SOLSR<sub>r</sub> models reduced the risk of over-fitting the prediction models<sup>42,43</sup>. There were more than six variables in all the SOLSR models, which may increase the difficulty of data interpretation and induce high variance in model simulations<sup>41,44,45</sup>. This may account for the lower prediction efficiencies in WCW by the SOLSR models than by the SPCR models.

Topography- based SPCR models have advantages in simulating soil redistribution and associated SOC dynamics. First, topographic information can be easily derived from DEMs. Recent increased accessibility of the high spatial resolution LiDAR data can help improve the accuracy of DEM-derived landscape topography and benefit investigations in regions with limited field observations. Second, using a set of topographic metrics and statistical analyses, the topography-based models can efficiently quantify soil redistribution and SOC distribution patterns. Third, the application of principal component can effectively reduce biases associated with multicollinearity of topographic metrics and increase the stability of the stepwise regression models when applied to multiple spatial scales.

However, the SPCA models may be limited by variables during model development. Although application of the LiDAR data increased in ecological studies, the methods to derive useful topographic information have not yet been fully explored. In this study, the TWI and LsRe showed the highest correlations with SOC density and soil redistribution rates, respectively. However, additional topographic variables that are not considered may be equally or more important in explaining soil erosion and C dynamics. Additionally, other factors such as management practices, which may cause soil erosion variability, were not included in this study. For example, when tillage was parallel to the direction of maximum slope, soil erosion may double relative to the erosion in slantwise tillage turning soil upslope<sup>46</sup>. Therefore, different tillage practices may also be a reason for the reduced prediction efficiencies of the SPCR models.

The study is based on the paper published in Catena<sup>17</sup>. Instead of a mechanistic-based analysis of topographic influences on soil movement and soil properties as performed in the Catena paper, here we focused on the methods for quantifying topographic metrics and developing topography-based models. We discussed the feasibility and advantages of using topography-based models in studies of the spatial structure of soil properties. Meanwhile, we improved our models by updating algorithms of slope length factor and flow accumulation. The scale of slope length factor measurement was limited to field's area. Additionally, the deterministic infinity algorithm was used for flow accumulation generation. Compared with the method reported in Li *et al.*<sup>17</sup> which generated flow accumulation with a deterministic eight-node algorithm, the infinity algorithm adopted in this study reduces loops in the flow direction angles and proved to be a better algorithm for low relief areas<sup>47</sup>.

In conclusion, our results demonstrate the feasibility of topography-based SPCR models in simulating SOC distribution and soil redistribution patterns in agriculture fields. As a cost-effective method to estimate SOC stocks and soil redistribution rates, it is applicable to sites with limited observational data and private lands lacking public access. In future studies, the

prediction models could be improved with further refinement and availability of LiDAR data and inclusion of additional topographic metrics. The large-scale soil property maps that were developed based on the models will lead to further understanding of the mechanisms underlying the topographic impacts on soil movement in agricultural landscapes and the fate of SOC at the watershed and regional scales.

#### ACKNOWLEDGMENTS:

This research was supported by the USDA Natural Resources Conservation Service in association with the Wetland Component of the National Conservation Effects Assessment Project (NRCS 67-3A75-13-177).

#### DISCLOSURES:

The authors have nothing to disclose.

#### REFERENCES:

1. Lal, R. Soil erosion and carbon dynamics. *Soil and Tillage Research*. **81** (2), 137–142 (2005).
2. Fox, J. F., Papanicolaou, A. N. The use of carbon and nitrogen isotopes to study watershed erosion processes. *Journal of the American Water Resources Association*. **43** (4), 1047–1064 (2007).
3. Hemelryck, H. V., Fiener, P., Van Oost, K., Govers, G., Merckx, R. The effect of soil redistribution on soil organic carbon: An experimental study. *Biogeosciences*. **7** (12), 3971–3986 (2010).
4. McCarty, G. W., Ritchie, J. C. Impact of soil movement on carbon sequestration in agricultural ecosystems. *Environmental Pollution*. **116** (3), 423–430 (2002).
5. Quine, T. A., van Oost, K. Quantifying carbon sequestration as a result of soil erosion and deposition: Retrospective assessment using caesium-137 and carbon inventories. *Global Change Biology*. **13** (12), 2610–2625 (2007).
6. Polyakov, V. O., Lal, R. Soil organic matter and CO<sub>2</sub> emission as affected by water erosion on field runoff plots. *Geoderma*. **143** (1–2), 216–222 (2008).
7. Balesdent, J., Mariotti, A., Boissgonier, D. Effect of tillage on soil organic carbon mineralization estimated from <sup>13</sup>C abundance in maize fields. *Journal of Soil Science*. **41**, 587–596 (1990).
8. Van Oost, K., *et al.* Landscape-scale modeling of carbon cycling under the impact of soil redistribution: The role of tillage erosion. *Global Biogeochemical Cycles*. **19** (4), 1–13 (2005).
9. De Gryze, S., Six, J., Bossuyt, H., Van Oost, K., Merckx, R. The relationship between landform and the distribution of soil C, N and *p* under conventional and minimum tillage. *Geoderma*. **144** (1–2), 180–188 (2008).
10. Zhang, J., Quine, T. A., Ni, S., Ge, F. Stocks and dynamics of SOC in relation to soil redistribution by water and tillage erosion. *Global Biogeochemical Cycles*. **12**, 1834–1841 (2006).
11. Ritchie, J. C., McCarty, G. W., Venteris, E. R., Kaspar, T. C. Soil and soil organic carbon redistribution on the landscape. *Geomorphology*. **89**, 163–171 (2007).
12. Van der Perk, M., Slávik, O., Fulajtár, E. Assessment of spatial variation of cesium-137 in

- small catchments. *Journal of Environmental Quality*. **31** (6), 1930–1939 (2002).
13. Rezaei, S. A., Gilkes, R. J. The effects of landscape attributes and plant community on soil physical properties in rangelands. *Geoderma*. **125** (1–2), 145–154 (2005).
  14. Rieke-Zapp, D. H., Nearing, M. A. Slope shape effects on erosion: a laboratory study. *Soil Science Society of America Journal*. **69** (5), 1463–1471 (2005).
  15. Schwanghart, W., Jarmer, T. Linking spatial patterns of soil organic carbon to topography - A case study from south-eastern Spain. *Geomorphology*. **126** (1–2), 252–263 (2011).
  16. Dialynas, Y. G., *et al.* Topographic variability and the influence of soil erosion on the carbon cycle. *Global Biogeochemical Cycles*. **30**, 644–660 (2016).
  17. Li, X., McCarty, G. W., Karlen, D. L., Cambardella, C. A. Topographic metric predictions of soil redistribution and organic carbon in Iowa cropland fields. *Catena*. **160**, 222–232 (2018).
  18. Amore, E., Modica, C., Nearing, M. A., Santoro, V. C. Scale effect in USLE and WEPP application for soil erosion computation from three Sicilian basins. *Journal of Hydrology*. **293** (1–4), 100–114 (2004).
  19. Doetterl, S., *et al.* Erosion, deposition and soil carbon: A review of process-level controls, experimental tools and models to address C cycling in dynamic landscapes. *Earth-Science Reviews*. **154**, 102–122 (2016).
  20. Gessler, P. E., Chadwick, O. A., Chamran, F., Althouse, L., Holmes, K. Modeling soil–landscape and ecosystem properties using terrain attributes. *Soil Science Society of America Journal*. **64** (6), 2046–2056 (2000).
  21. Montgomery, D. R., Brandon, M. T. Topographic controls on erosion rates in tectonically active mountain ranges. *Earth and Planetary Science Letters*. **201** (3–4), 481–489 (2002).
  22. Pan, B., Geng, H., Hu, X., Sun, R., Wang, C. The topographic controls on the decadal-scale erosion rates in Qilian Shan Mountains, N.W. China. *Earth and Planetary Science Letters*. **292** (1–2), 148–157 (2010).
  23. Conrad, O., *et al.* System for Automated Geoscientific Analyses (SAGA) v . 2 .1.4. *Geoscientific Model Development*. **8**, 1991–2007 (2015).
  24. Walling, D. E., Zhang, Y., He, Q. Models for deriving estimates of erosion and deposition rates from fallout radionuclide (caesium-137, excess lead-210, and beryllium-7) measurements and the development of user friendly software for model implementation (IAEA-TECDOC-1665). *International Atomic Energy Agency*. 11–33 (2011).
  25. Sindayihebura, A., Ottoy, S., Dondeyne, S., Meirvenne, M. Van, Orshoven, J. Van. Comparing digital soil mapping techniques for organic carbon and clay content : Case study in Burundi’s central plateaus. *Catena*. **156**, 161–175 (2017).
  26. Schumacher, J. A., Kaspar, T. C., Ritchie, J. C., Schumacher, T. E., Karlen, D. L. Identifying spatial patterns of erosion for use in precision conservation. *Journal of Soil and Water Conservation*. **60** (6), 355–362 (2005).
  27. Young, C. J., *et al.* Evaluation of a model framework to estimate soil and soil organic carbon redistribution by water and tillage using <sup>137</sup>Cs in two U.S. Midwest agricultural fields. *Geoderma*. **232**, 437–448 (2014).
  28. Afshar, F. A., Ayoubi, S., Jalalian, A. Soil redistribution rate and its relationship with soil organic carbon and total nitrogen using <sup>137</sup>Cs technique in a cultivated complex hillslope in western Iran. *Journal of Environmental Radioactivity*. **101** (8), 606–614 (2010).

- 529 29. Li, Q. Y., Fang, H. Y., Sun, L. Y., Cai, Q. G. Using the  $^{137}\text{Cs}$  technique to study the effect of  
530 soil redistribution on soil organic carbon and total nitrogen stocks in an agricultural  
531 catchment of Northeast China. *Land Degradation & Development*. **25** (4), 350–359 (2014).
- 532 30. Troch, P., Van Loon, E., Hilberts, A. Analytical solutions to a hillslope-storage kinematic  
533 wave equation for subsurface flow. *Advances in Water Resources*. **25** (6), 637–649 (2002).
- 534 31. Tucker, G. E., Bras, R. L. Hillslope processes, drainage density, and landscape morphology.  
535 *Water Resources Research*. **34** (10), 2751–2764 (1998).
- 536 32. Seijmonsbergen, A. C., Hengl, T., Anders, N. S. Semi-Automated Identification and  
537 Extraction of Geomorphological Features Using Digital Elevation Data. *Developments in*  
538 *Earth Surface Processes*. **15**, (2011).
- 539 33. Moore, I. D., Grayson, R. B., Ladson, D. A. R. Digital terrain modelling: A review of  
540 hydrological, geomorphological, and biological applications. *Hydrological Processes*. **5**, 3–  
541 30 (1991).
- 542 34. Kirkby, M. J. Do not only connect: A model of infiltration-excess overland flow based on  
543 simulation. *Earth Surface Processes and Landforms*. **39** (7), 952–963 (2014).
- 544 35. Sharpley, A., Kleinman, P. Effect of rainfall simulator and plot scale on overland flow and  
545 phosphorus transport. *Journal of Environmental Quality*. **32** (6), 2172–2179 (2003).
- 546 36. Hjerdt, K. N. A new topographic index to quantify downslope controls on local drainage.  
547 *Water Resources Research*. **40** (5), 1–6 (2004).
- 548 37. Kasai, M., Marutani, T., Reid, L. M., Trustrum, N. A. Estimation of temporally averaged  
549 sediment delivery ratio using aggradational terraces in headwater catchments of the  
550 Waipaoa River, North Island, New Zealand. *Earth Surface Processes and Landforms*. **26** (1),  
551 1–16 (2001).
- 552 38. Lang, M. W., McCarty, G. W., Oesterling, R., Yeo, I. Y. Topographic metrics for improved  
553 mapping of forested wetlands. *Wetlands*. **33** (1), 141–155 (2013).
- 554 39. Li, X., *et al.* Topographic and physicochemical controls on soil denitrification in prior  
555 converted croplands located on the Delmarva Peninsula, USA. *Geoderma*. **309**, 41–49  
556 (2018).
- 557 40. Conforti, M., Aucelli, P. P. C., Robustelli, G., Scarciglia, F. Geomorphology and GIS analysis  
558 for mapping gully erosion susceptibility in the Turbolo stream catchment (Northern  
559 Calabria, Italy). *Natural Hazards*. **56** (3), 881–898 (2011).
- 560 41. Dormann, C. F., *et al.* Collinearity: A review of methods to deal with it and a simulation  
561 study evaluating their performance. *Ecography*. **36** (1), 027–046 (2013).
- 562 42. Fodor, I. K. A survey of dimension reduction techniques. *Center for Applied Scientific*  
563 *Computing, Lawrence Livermore National Laboratory*. **9**, 1–18 (2002).
- 564 43. Quijano, L., Gaspar, L., Navas, A. Spatial patterns of SOC, SON,  $^{137}\text{Cs}$  and soil properties  
565 as affected by redistribution processes in a Mediterranean cultivated field (Central Ebro  
566 Basin). *Soil and Tillage Research*. **155**, 318–328 (2016).
- 567 44. Næs, T., Martens, H. Principal component regression in NIR analysis: Viewpoints,  
568 background details and selection of components. *Journal of Chemometrics*. **2** (2), 155–167  
569 (1988).
- 570 45. Shlens, J. A Tutorial on Principal Component Analysis. *Measurement*. **51**, 52 (2014).
- 571 46. Heckrath, G., *et al.* Tillage erosion and its effect on soil properties and crop yield in  
572 Denmark. *Journal of Environmental Quality*. **34**, 312–324 (2005).

- 573 47. Tarboron, G. A new method for the determination of flow directions and upslope areas in  
574 grid digital elevation models. *Water Resources Research*. **33** (2), 309–319 (1997).  
575



[Click here to download Figure Figure1\\_2.tif](#) 



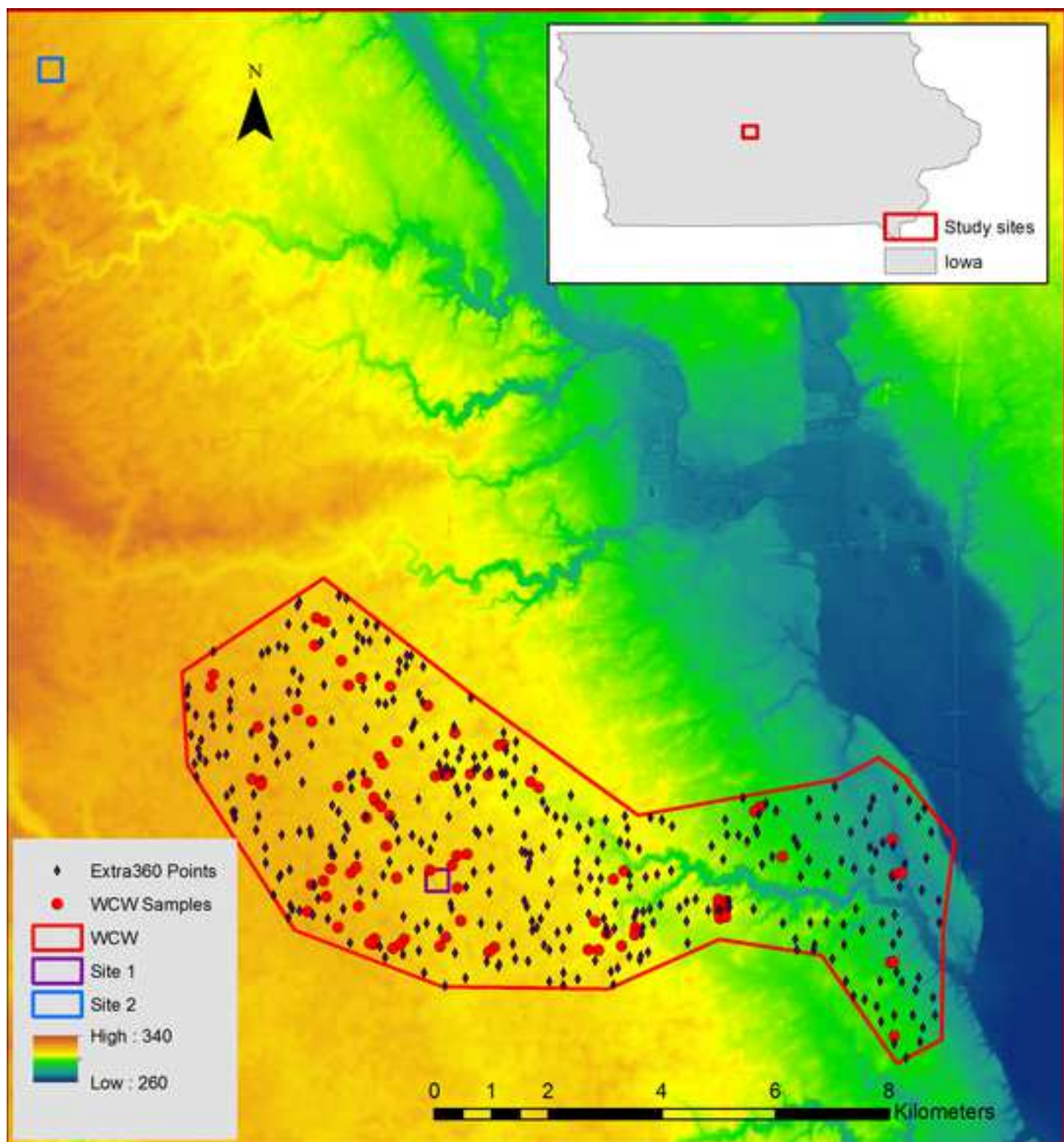


Figure 3

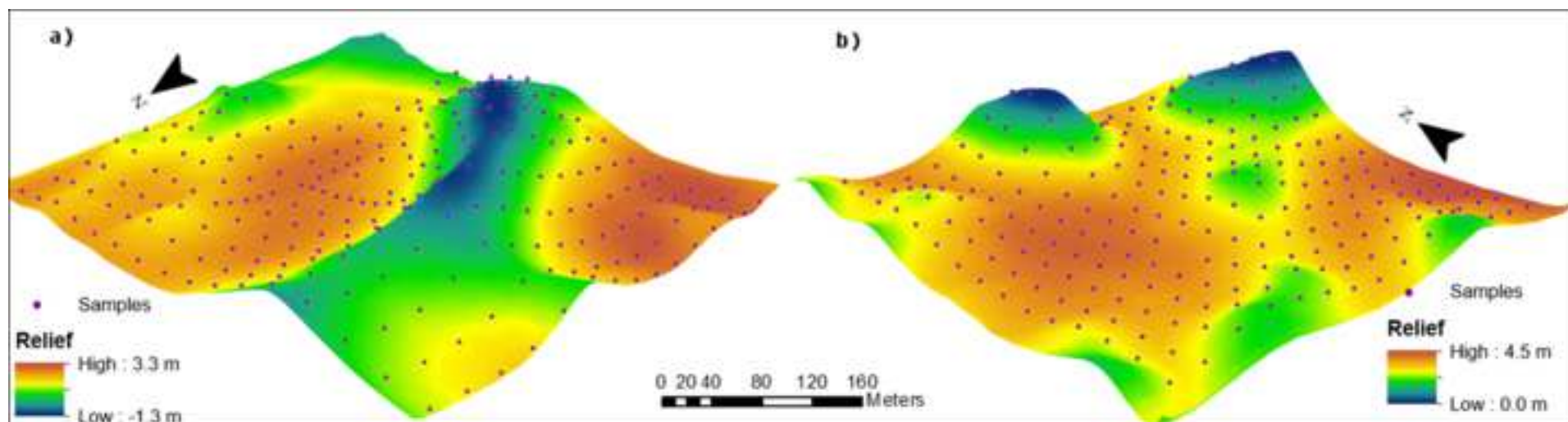




Figure 4

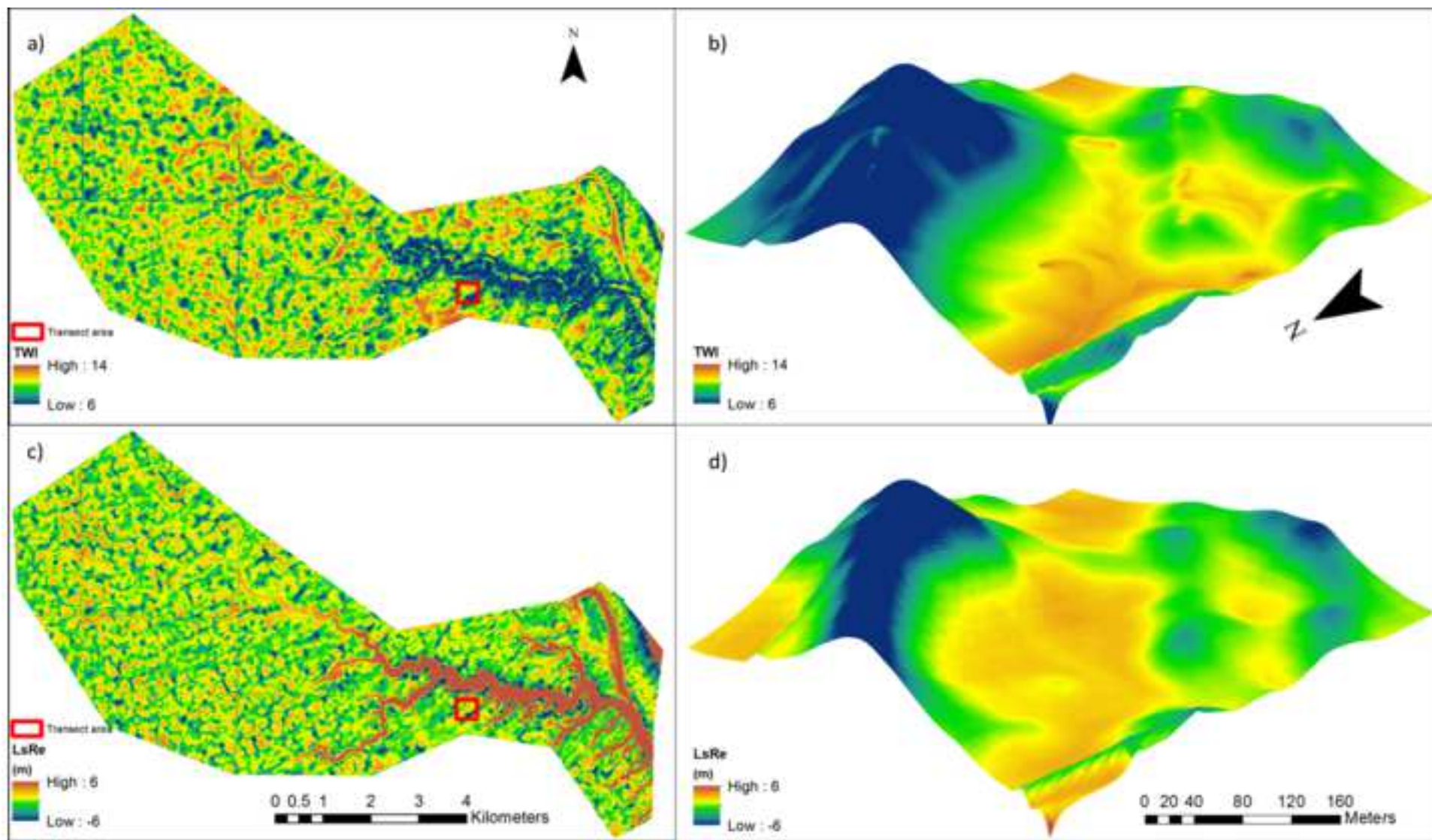
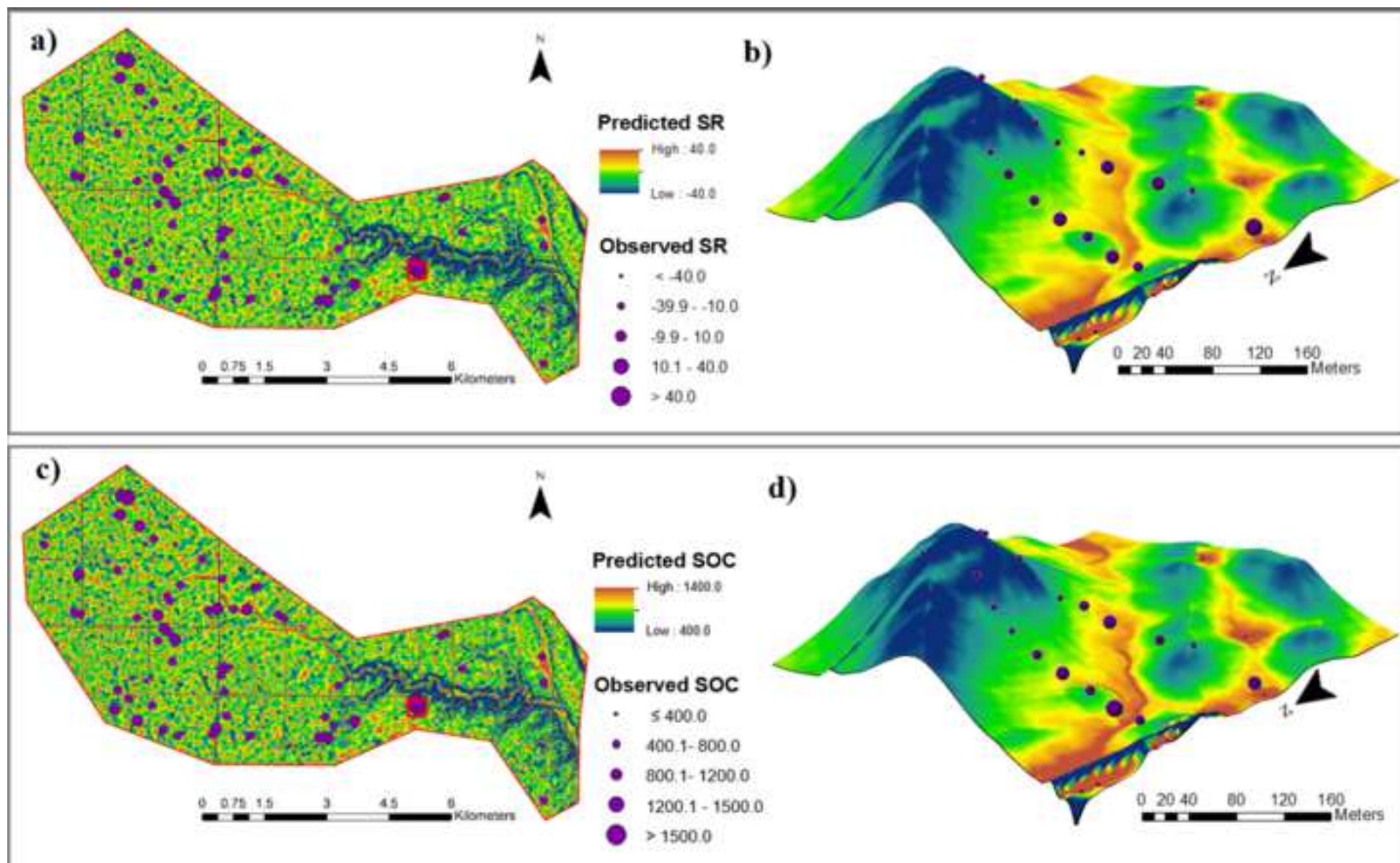


Figure 5



Variables
Slope (radian)
Profile Curvature ( $m^{-1}$ )
Plan Curvature ( $m^{-1}$ )
General Curvature ( $m^{-1}$ )
Flow accumulation
Topographic Relief (m)
Positive Openness (radian)
Upslope Slope (m)
Flow Path Length (m)
Downslope Index (radian)
Catchment Area ( $m^2$ )
Topographic Wetness Index
Stream Power Index
Slope Length Factor

---

## Significance

---

Runoff velocity, soil water content<sup>28,29</sup>

Flow acceleration, soil erosion, deposition rate<sup>11,30</sup>

Flow convergence and divergence, soil water content<sup>30</sup>

Runoff velocity , soil erosion, deposition<sup>29</sup>

Soil water content, runoff volume<sup>20</sup>

Landscape drainage characteristics, runoff velocity and acceleration<sup>21,31</sup>

Landscape drainage characteristics , soil water content<sup>32</sup>

Runoff velocity<sup>33,34</sup>

Sediment yield, erosion rate<sup>35</sup>

Soil water content<sup>36</sup>

Runoff velocity and volume<sup>33,37</sup>

Soil moisture distribution<sup>28,38,39</sup>

Soil erosion, Convergence of flow<sup>40</sup>

Flow convergence and divergence<sup>28,40</sup>

---

	Slope (radian)	P_Cur (m <sup>-1</sup> )	Pl_Cur (m <sup>-1</sup> )	G_Cur (m <sup>-1</sup> )	FA	LsRe (m)	SsRe (m)	POP (radian)
SOC	-0.687 ***,†	-0.159 **	-0.333 ***	-0.288 ***	0.165 ***	0.698 ***,†	-0.171 ***	-0.451 ***
SR	-0.65 ***,†	-0.205 ***	-0.274 ***	-0.282 ***	0.156 **	0.687 ***,‡	-0.099 *	-0.427 ***

P\_Cur, Pl\_Cur, and G\_Cur are profile curvature, plan curvature and general curvature, respectively; FA is

\* P < 0.05, \*\* P < 0.005, \*\*\* P < 0.0001.

†Correlation coefficient >0.5, ‡Highest correlation coefficient for each soil property.



Upl (m)	FPL (m)	DI (°)	CA (m <sup>2</sup> )	TWI	SPI	LS_FB
-0.315 ***	0.499 ***	0.413 ***	0.588 ***,†	0.735 ***,‡	0.165 ***	-0.453 ***
-0.217 ***	0.487 ***	0.361 ***	0.565 ***,†	0.647 ***,†	0.156 ***	-0.438 ***

s flow accumulation; RePC1 and RePC2 are topographic relief component 1 and 2, respectively; POP100

is positive openness; Upsl is upslope slope; FPL is flow path length; DI is downslope index; CA is catchment area

ent area; TWI is topographic wetness index; and SPI is stream power index; and LS\_FB is slope length fac

tor (field based).

	PC1(25%)	PC2(24%)	PC3(14%)	PC6(5%)	PC7(4%)
Slope	0.062	0.475†	-0.035	-0.013	-0.183
P_Cur	-0.290	0.000	0.346	-0.070	-0.002
Pl_Cur	-0.283	0.107	-0.001	0.485†	0.383†
G_Cur	-0.353†	0.054	0.275	0.025	0.100
FA	0.297	-0.042	0.482†	0.179	0.131
LsRe	0.309	-0.193	-0.237	0.113	-0.116
SsRe	0.234	0.266	-0.118	0.084	0.597†
POP100	-0.330	0.092	0.258	-0.292	0.217
Upsl	0.187	0.419†	-0.143	-0.066	0.012
FPL	0.147	-0.168	-0.088	-0.703†	0.407†
DI	0.103	-0.220	-0.164	0.184	0.435†
CA	0.326	-0.128	0.4†	-0.160	-0.092
TWI	0.053	-0.465†	-0.067	0.185	-0.047
SPI	0.345	-0.014	0.46†	0.169	0.080
LS_FB	0.256	0.396†	0.050	0.011	-0.072

P\_Cur, Pl\_Cur, and G\_Cur are profile curvature, plan curvature and general curvature, respectively; FA i:

†Loadings> 0.35.

s flow accumulation; RePC1 and RePC2 are topographic relief component 1 and 2, respectively; POP100

is positive openness; Upsl is upslope slope; FPL is flow path length; DI is downslope index; CA is catchment area

ent area; TWI is topographic wetness index; and SPI is stream power index; and LS\_FB is slope length fa



ctor (field based).

Stepwise principal component regression (SPCR)
SOC
SR
Stepwise ordinary least square regression (SOLSR <sub>f</sub> )
SOC
SR
Stepwise ordinary least square regression with collinear covariate removed (SOLSR <sub>r</sub> )
SOC
SR

† The order of TPCs is based on the stepwise selection steps

R<sup>2</sup><sub>adj</sub> is adjusted coefficient of determination; NSE is Nash-Sutcliffe efficiency; RSR is ratio

PC represents principal component. TWI is topographic wetness index; FPL is flow path le

Model	$R^2_{adj}$
2.932-0.058TPC2-0.025TPC3+0.051TPC7+0.037TPC1+	0.68
2.111+0.013TPC1+0.032TPC7-0.028TPC2-0.016TPC3-0.010TPC6	0.63
2.755+0.021TWI+0.0004FPL-6.369G_Cur-5.580Slope+	0.7
0.011LsRe+0.091DI+0.013SsRe+0.125LS_FB	
2.117+0.007LsRe-3.128Slope+0.109DI+0.010SsRe+0.0002FPL+ 0.801Upsl -4.442P_Cur	0.65
2.951+0.033LsRe-2.869Upsl+0.0006FPL+0.028SsRe+0.124DI-0.163LS_FB+0.007SPI-	0.68
10.187P_Cur	
2.042+0.016LsRe-0.146LS_FB+0.118DI+0.017SsRe+0.0003FPL+ 0.070POP	0.63

of the root mean square error (RMSE) to the standard deviation of measured data.

length; P\_Cur, Pl\_Cur, and G\_Cur are profile curvature, plan curvature and general curvature, respectively; LS\_

NSE	RSR
0.69	0.56
0.63	0.61
0.71	0.55
0.65	0.59
0.68	0.56
0.64	0.6

\_FB is slope length factor (field based); LsRe and SsRe are large-scale and small-scale topographic reliefs, res

spectively; DI is downslope index; and Upsl is upslope slope.

Name of Material/ Equipment	Company	Catalog Number	Comments/Description
Light Detection and Ranging (LiDAR) data		<a href="http://www.geotree.uni.edu/lidar/">http://www.geotree.uni.edu/lidar/</a>	Collected from the GeoTREE LiDAR mapping project
LECO CNS 2000 elemental analyzer	LECO Corp., St. Joseph, MI		
Canberra Genie-2000 Spectroscopy System	CANBERRA Industries		
Geographic positioning system	Trimble	RTK 4700 GPS	
ArcGIS	ESRI, Redlands, CA	10.2.2	
Statistical Analysis System	SAS Institute Inc		
System for Automated Geoscientific Analysis	University of Göttingen, Germany	v. 2.2.5, <a href="http://www.saga-gis.org/">http://www.saga-gis.org/</a>	GNU General Public License



1 Alawafa Center #200  
 Cambridge, MA 02140  
 Tel. 617.945.9051  
 www.jove.com

## ARTICLE AND VIDEO LICENSE AGREEMENT

Title of Article:

Use of Principal Components for Scaling Up Topographic Models to Map Soil Redistribution and Soil Organic Carbon

Author(s):

Xia Li, Gregory W. McCarty

Item 1 (check one box): The Author elects to have the Materials be made available (as described at <http://www.jove.com/author>) via: ☐ Standard Access ☒ Open Access

Item 2 (check one box):

- ☐ The Author is NOT a United States government employee.
- ☒ The Author is a United States government employee and the Materials were prepared in the course of his or her duties as a United States government employee.
- ☐ The Author is a United States government employee but the Materials were NOT prepared in the course of his or her duties as a United States government employee.

### ARTICLE AND VIDEO LICENSE AGREEMENT

1. **Defined Terms.** As used in this Article and Video License Agreement, the following terms shall have the following meanings: “**Agreement**” means this Article and Video License Agreement; “**Article**” means the article specified on the last page of this Agreement, including any associated materials such as texts, figures, tables, artwork, abstracts, or summaries contained therein; “**Author**” means the author who is a signatory to this Agreement; “**Collective Work**” means a work, such as a periodical issue, anthology or encyclopedia, in which the Materials in their entirety in unmodified form, along with a number of other contributions, constituting separate and independent works in themselves, are assembled into a collective whole; “**CRC License**” means the Creative Commons Attribution-Non Commercial-No Derivs 3.0 Unported Agreement, the terms and conditions of which can be found at: <http://creativecommons.org/licenses/by-nc-nd/3.0/legalcode>; “**Derivative Work**” means a work based upon the Materials or upon the Materials and other pre-existing works, such as a translation, musical arrangement, dramatization, fictionalization, motion picture version, sound recording, art reproduction, abridgment, condensation, or any other form in which the Materials may be recast, transformed, or adapted; “**Institution**” means the institution, listed on the last page of this Agreement, by which the Author was employed at the time of the creation of the Materials; “**JoVE**” means MyJove Corporation, a Massachusetts corporation and the publisher of *The Journal of Visualized Experiments*; “**Materials**” means the Article and / or the Video; “**Parties**” means the Author and JoVE; “**Video**” means any video(s) made by the Author, alone or in conjunction with any other parties, or by JoVE or its affiliates or agents, individually or in collaboration with the Author or any other parties, incorporating all or any portion of the Article, and in which the Author may or may not appear.

2. **Background.** The Author, who is the author of the Article, in order to ensure the dissemination and protection of the Article, desires to have the JoVE publish the Article and create and transmit videos based on the Article. In furtherance of such goals, the Parties desire to memorialize in this Agreement the respective rights of each Party in and to the Article and the Video.

3. **Grant of Rights in Article.** In consideration of JoVE agreeing to publish the Article, the Author hereby grants to JoVE, subject to **Sections 4 and 7** below, the exclusive, royalty-free, perpetual (for the full term of copyright in the Article, including any extensions thereto) license (a) to publish, reproduce, distribute, display and store the Article in all forms, formats and media whether now known or hereafter developed (including without limitation in print, digital and electronic form) throughout the world, (b) to translate the Article into other languages, create adaptations, summaries or extracts of the Article or other Derivative Works (including, without limitation, the Video) or Collective Works based on all or any portion of the Article and exercise all of the rights set forth in (a) above in such translations, adaptations, summaries, extracts, Derivative Works or Collective Works and (c) to license others to do any or all of the above. The foregoing rights may be exercised in all media and formats, whether now known or hereafter devised, and include the right to make such modifications as are technically necessary to exercise the rights in other media and formats. If the “Open Access” box has been checked in **Item 1** above, JoVE and the Author hereby grant to the public all such rights in the Article as provided in, but subject to all limitations and requirements set forth in, the CRC License.

## ARTICLE AND VIDEO LICENSE AGREEMENT

4. **Retention of Rights in Article.** Notwithstanding the exclusive license granted to JoVE in **Section 3** above, the Author shall, with respect to the Article, retain the non-exclusive right to use all or part of the Article for the non-commercial purpose of giving lectures, presentations or teaching classes, and to post a copy of the Article on the Institution's website or the Author's personal website, in each case provided that a link to the Article on the JoVE website is provided and notice of JoVE's copyright in the Article is included. All non-copyright intellectual property rights in and to the Article, such as patent rights, shall remain with the Author.

5. **Grant of Rights in Video – Standard Access.** This **Section 5** applies if the "Standard Access" box has been checked in **Item 1** above or if no box has been checked in **Item 1** above. In consideration of JoVE agreeing to produce, display or otherwise assist with the Video, the Author hereby acknowledges and agrees that, Subject to **Section 7** below, JoVE is and shall be the sole and exclusive owner of all rights of any nature, including, without limitation, all copyrights, in and to the Video. To the extent that, by law, the Author is deemed, now or at any time in the future, to have any rights of any nature in or to the Video, the Author hereby disclaims all such rights and transfers all such rights to JoVE.

6. **Grant of Rights in Video – Open Access.** This **Section 6** applies only if the "Open Access" box has been checked in **Item 1** above. In consideration of JoVE agreeing to produce, display or otherwise assist with the Video, the Author hereby grants to JoVE, subject to **Section 7** below, the exclusive, royalty-free, perpetual (for the full term of copyright in the Article, including any extensions thereto) license (a) to publish, reproduce, distribute, display and store the Video in all forms, formats and media whether now known or hereafter developed (including without limitation in print, digital and electronic form) throughout the world, (b) to translate the Video into other languages, create adaptations, summaries or extracts of the Video or other Derivative Works or Collective Works based on all or any portion of the Video and exercise all of the rights set forth in (a) above in such translations, adaptations, summaries, extracts, Derivative Works or Collective Works and (c) to license others to do any or all of the above. The foregoing rights may be exercised in all media and formats, whether now known or hereafter devised, and include the right to make such modifications as are technically necessary to exercise the rights in other media and formats. For any Video to which this Section 6 is applicable, JoVE and the Author hereby grant to the public all such rights in the Video as provided in, but subject to all limitations and requirements set forth in, the CRC License.

7. **Government Employees.** If the Author is a United States government employee and the Article was prepared in the course of his or her duties as a United States government employee, as indicated in **Item 2** above, and any of the licenses or grants granted by the Author hereunder exceed the scope of the 17 U.S.C. 403, then the rights granted hereunder shall be limited to the maximum rights permitted under such

statute. In such case, all provisions contained herein that are not in conflict with such statute shall remain in full force and effect, and all provisions contained herein that do so conflict shall be deemed to be amended so as to provide to JoVE the maximum rights permissible within such statute.

8. **Likeness, Privacy, Personality.** The Author hereby grants JoVE the right to use the Author's name, voice, likeness, picture, photograph, image, biography and performance in any way, commercial or otherwise, in connection with the Materials and the sale, promotion and distribution thereof. The Author hereby waives any and all rights he or she may have, relating to his or her appearance in the Video or otherwise relating to the Materials, under all applicable privacy, likeness, personality or similar laws.

9. **Author Warranties.** The Author represents and warrants that the Article is original, that it has not been published, that the copyright interest is owned by the Author (or, if more than one author is listed at the beginning of this Agreement, by such authors collectively) and has not been assigned, licensed, or otherwise transferred to any other party. The Author represents and warrants that the author(s) listed at the top of this Agreement are the only authors of the Materials. If more than one author is listed at the top of this Agreement and if any such author has not entered into a separate Article and Video License Agreement with JoVE relating to the Materials, the Author represents and warrants that the Author has been authorized by each of the other such authors to execute this Agreement on his or her behalf and to bind him or her with respect to the terms of this Agreement as if each of them had been a party hereto as an Author. The Author warrants that the use, reproduction, distribution, public or private performance or display, and/or modification of all or any portion of the Materials does not and will not violate, infringe and/or misappropriate the patent, trademark, intellectual property or other rights of any third party. The Author represents and warrants that it has and will continue to comply with all government, institutional and other regulations, including, without limitation all institutional, laboratory, hospital, ethical, human and animal treatment, privacy, and all other rules, regulations, laws, procedures or guidelines, applicable to the Materials, and that all research involving human and animal subjects has been approved by the Author's relevant institutional review board.

10. **JoVE Discretion.** If the Author requests the assistance of JoVE in producing the Video in the Author's facility, the Author shall ensure that the presence of JoVE employees, agents or independent contractors is in accordance with the relevant regulations of the Author's institution. If more than one author is listed at the beginning of this Agreement, JoVE may, in its sole discretion, elect not take any action with respect to the Article until such time as it has received complete, executed Article and Video License Agreements from each such author. JoVE reserves the right, in its absolute and sole discretion and without giving any reason therefore, to accept or decline any work submitted to JoVE. JoVE and its employees, agents and independent contractors shall have



## ARTICLE AND VIDEO LICENSE AGREEMENT

full, unfettered access to the facilities of the Author or of the Author's institution as necessary to make the Video, whether actually published or not. JoVE has sole discretion as to the method of making and publishing the Materials, including, without limitation, to all decisions regarding editing, lighting, filming, timing of publication, if any, length, quality, content and the like.

11. **Indemnification.** The Author agrees to indemnify JoVE and/or its successors and assigns from and against any and all claims, costs, and expenses, including attorney's fees, arising out of any breach of any warranty or other representations contained herein. The Author further agrees to indemnify and hold harmless JoVE from and against any and all claims, costs, and expenses, including attorney's fees, resulting from the breach by the Author of any representation or warranty contained herein or from allegations or instances of violation of intellectual property rights, damage to the Author's or the Author's institution's facilities, fraud, libel, defamation, research, equipment, experiments, property damage, personal injury, violations of institutional, laboratory, hospital, ethical, human and animal treatment, privacy or other rules, regulations, laws, procedures or guidelines, liabilities and other losses or damages related in any way to the submission of work to JoVE, making of videos by JoVE, or publication in JoVE or elsewhere by JoVE. The Author shall be responsible for, and shall hold JoVE harmless from, damages caused by lack of sterilization, lack of cleanliness or by contamination due to the making of a video by JoVE its employees, agents or independent contractors. All sterilization, cleanliness or decontamination procedures shall be solely the responsibility of the Author and shall be undertaken at the Author's


expense. All indemnifications provided herein shall include JoVE's attorney's fees and costs related to said losses or damages. Such indemnification and holding harmless shall include such losses or damages incurred by, or in connection with, acts or omissions of JoVE, its employees, agents or independent contractors.

12. **Fees.** To cover the cost incurred for publication, JoVE must receive payment before production and publication the Materials. Payment is due in 21 days of invoice. Should the Materials not be published due to an editorial or production decision, these funds will be returned to the Author. Withdrawal by the Author of any submitted Materials after final peer review approval will result in a US\$1,200 fee to cover pre-production expenses incurred by JoVE. If payment is not received by the completion of filming, production and publication of the Materials will be suspended until payment is received.

13. **Transfer, Governing Law.** This Agreement may be assigned by JoVE and shall inure to the benefits of any of JoVE's successors and assignees. This Agreement shall be governed and construed by the internal laws of the Commonwealth of Massachusetts without giving effect to any conflict of law provision thereunder. This Agreement may be executed in counterparts, each of which shall be deemed an original, but all of which together shall be deemed to me one and the same agreement. A signed copy of this Agreement delivered by facsimile, e-mail or other means of electronic transmission shall be deemed to have the same legal effect as delivery of an original signed copy of this Agreement.

A signed copy of this document must be sent with all new submissions. Only one Agreement required per submission.

### CORRESPONDING AUTHOR:

Name:	Gregory W. McCarty	
Department:		
Institution:	USDA-ARS	
Article Title:	Use of Principal Components for Scaling Up Topographic Models to Map Soil Redistribution and Soil Organic Carbon	
Signature:		Date: 3/22/18

Please submit a **signed** and **dated** copy of this license by one of the following three methods:

- 1) Upload a scanned copy of the document as a pdf on the JoVE submission site;
- 2) Fax the document to +1.866.381.2236;
- 3) Mail the document to JoVE / Attn: JoVE Editorial / 1 Alewife Center #200 / Cambridge, MA 02139

For questions, please email [submissions@jove.com](mailto:submissions@jove.com) or call +1.617.945.9051

**Editorial comments:**

We appreciate the Editor for his/her insightful comments. We have revised and improved the manuscript according to the valuable suggestions.

*1. Figures 2 and 3 look to be substantially the same as Figure 1 in your Catena paper; as that is under a CC license, permission is not necessary, but you must cite it in the Figure legends.*

**RESPONSE:** We added the citation in the legends of Figures 2 and 3.

*2. Step 3 will be very difficult to script and film, in particular without explicit software steps. Please provide more detail or do not highlight.*

**RESPONSE:** We added more details in Step 3. With all these steps, we hope that it is sufficient to repeat the model development procedure. Please let us know if more information is needed.

*3. 3.1.5: Should this be 'Variance' Inflation Factor?*

**RESPONSE:** We changed into "Variance".

*4. Table 1: Please remove the references and ensure that the citations match up with the references list in the manuscript.*

**RESPONSE:** We removed the references from table and added to the reference list.

*5. Per your response to Reviewer 1, can you more explicitly say which data was used to calibrate the model and which data to validate? It's not apparent in the current manuscript.*

**RESPONSE:** In this study, we collected soil samples from two spatial scales, including large-scale (watershed scale) and small-scale (site scale). The SOC density and soil redistribution rates from soil samples collected from the two field sites were used for model calibration. Soil data collected from the watershed area were used for model validation. We've added the information in the manuscript.

**Thank you for all these valuable comments**